# Trapping effects on the vibration-inversion-rotation motions of an ammonia molecule encapsulated in $C_60$ fullerene molecule.

Azzedine Lakhlifi*

Institut UTINAM-UMR CNRS 6213 Université de Franche-Comté
Observatoire de Besançon
41 bis avenue de l'Observatoire - BP 1615 - 25010 Besançon Cedex, France
and Pierre R. Dahoo
CNRS-INSU, LATMOS-IPSL - Université de Versailles
11 Bd d'Alembert - 78820 Guyancourt, France

March 30, 2011

**Abstract**

The infrared bar-spectrum of a single ammonia molecule encapsulated in nano-cage $C_{60}$ fullerene molecule is modelled using the site inclusion model successfully applied to analyze spectra of $CO_2$ isotopologues isolated in rare gas matrix. Calculations show that $NH_3$ can rotate freely on a sphere of radius 0.184 Å around the site centre of the nano-cage and spin freely about its $C_3$ symmetry axis. In the static field inside the cage degenerate $\nu_3$ and $\nu_4$ vibrational modes are blue shifted and split. When dynamic coupling with translational motion is considered, the spectral signature of the $\nu_2$ mode is modified with a higher hindering barrier (2451 $cm^{-1}$), an effective reduced mass (6.569 $g.mol^{-1}$) and a longer tunneling time (55594 ps) for the fundamental level compared to gas-phase values (2047 $cm^{-1}$), (2.563 $g.mol^{-1}$) and (20.85 ps). As a result this mode is red shifted. Moreover, simulation shows that the changes in the bar-spectrum of the latter mode can be used to probe the temperature of the surrounding media in which fullerene is observed.

## 1 Introduction

Quite recently, "buckyballs" have been observed for the first time in space by Astronomers of University of Western Ontario [1, 2] using NASA's Spitzer Space Telescope. They identified spectral signatures of fullerenes in a cloud of cosmic dust surrounding a distant star 6500 light years away. The existence of fullerenes has thus been confirmed as anticipated after the first observation in laboratory by Kroto *et al.* at Rice University [3]. One may therefore expect observation of molecular species trapped in fullerenes in interstellar medium. In this work we investigate on the changes that are induced in the spectral signatures of species trapped in fullerene in order to determine how these changes can be used to characterize the environment where fullerenes are observed. From inert matrix isolation spectroscopy, one knows that infrared (IR) spectra of molecular species trapped in a site are simplified in that, as rotational structures are absent in the spectra, a vibrational transition is observed as one peak blue or red shifted or sometimes two or more in case of splitting of degenerate levels [4, 5, 6].

Trapping of atoms or ions and small diatomic molecules in fullerene have been studied both experimentally and theoretically [7, 8, 9, 10, 11, 12, 13, 14, 15, 16, 17, 18, 19, 20, 21, 22]. However, except for CO [17, 18, 19] and $H_2$ [20, 21] molecules, only a few of the theoretical work has been done in the infrared region. In the case of $NH_3$ trapped in fullerene, calculations have been performed from *ab-initio* methods to study the trapping mechanism [22, 23, 24] but no experimental work has been published.

*Institut Universitaire de Technologie, Belfort-Montbéliard. E-mail : azzedine.lakhlifi@obs-besancon.fr

Erkoç and Türker [23] have reported that up to six $NH_3$ molecules can be trapped in $C_{60}$, on one hand and Ganji *et al.* [24] suggest that only one $NH_3$ molecule can form a stable complex $NH_3@C_{60}$ on the other hand. While Slanina *et al.* [22] have reported a binding energy of -1830 $cm^{-1}$ with the ammonia molecule oriented towards a pair of parallel pentagons.

The aim of this paper is to determine how fullerene modifies the spectral signature of ammonia molecule, in particular in the region of the vibration-inversion mode (namely umbrella mode).

A theoretical study of an ammonia molecule trapped in fullerene $C_{60}$ is thus performed in order to simulate its infrared spectrum in the vibration-inversion frequency region. The choice of $NH_3$ is motivated by the fact that it contains a nitrogen atom. $CO_2$ could otherwise have been chosen for the simulation.

To simulate the infrared spectra of $NH_3$ in fullerene, we use the site inclusion model successfully applied to analyze spectra of $CO_2$ isotopologues [6] isolated in rare gas matrix. When the molecule is trapped in the nano-cage of fullerene, the interaction with carbon atoms in the short range scale modifies the translational and rotational degrees of freedom because the molecule is no longer free to move. As a result, the umbrella mode which is characterized by the inversion doubling through tunneling of the nitrogen atom across the plane defined by the three H atoms is perturbed as discussed below.

To calculate the bar-spectra of $NH_3$ trapped in $C_{60}$ nano-cage a renormalization procedure is applied on the total Hamiltonian of the system. The dynamical coupling between the molecular degrees of freedom and those of $C_{60}$ nano-cage is then small enough, at least to a first approximation, to justify an *initial chaos hypothesis*. As a result, the density matrix operator of the system can be factorized into a product consisting of two terms, one related to the $NH_3$ renormalized optical states and the other to the $C_{60}$ bath states spanned by its vibrational modes. The dynamical line-shifts and line-widths of the bar-spectra can be disregarded and $C_{60}$ nano-cage considered as rigid.

The interaction potential model used in our calculations is presented in section 2 and the renormalization method applied to separate the different motions from each other described. Results of the calculation to determine the frequency shifts of the vibrational modes and the orientational level schemes of the molecule are then given. Sections 3 and 4 are devoted to a presentation of the formalism used for the construction of the infrared spectra of $NH_3$ in fullerene and to a discussion of the infrared bar-spectrum in the frequency region of the $\nu_2$ mode.

# 2 The interaction potential energy

## 2.1 Potential energy model

The interaction potential energy $V_{\mathrm{MC}}$ between the trapped ammonia molecule $NH_3$ and the rigid fullerene molecule $C_{60}$ is modelled as the sum of 12-6 Lennard-Jones (LJ) pairwise atom-atom potentials characterizing the repulsion-dispersion contributions and the induction part due to the interaction between the permanent electric multipole moments of the molecule and their images created at the positions of the polarized fullerene carbon atoms. It can be expressed as

$$V_{\mathrm{MC}} = \sum_{j=1}^{60}\sum_{i=1}^{4} 4\epsilon_{ij}\left\{\left(\frac{\sigma_{ij}}{|\mathbf{r}_{ij}|}\right)^{12} - \left(\frac{\sigma_{ij}}{|\mathbf{r}_{ij}|}\right)^{6}\right\} - \frac{1}{2}\sum_{j=1}^{60}\mathbf{E}^{j}_{\mathrm{M}} : \alpha^{j} : \mathbf{E}^{j}_{\mathrm{M}}, \tag{1}$$

where $i$ and $j$ denote the $i$th atom of the ammonia molecule and the $j$th carbon atom of the fullerene molecule, respectively; $\epsilon_{ij}$ and $\sigma_{ij}$ are the mixed LJ potential parameters, obtained from the usual Lorentz-Berthelot combination rules $\epsilon_{ij} = \sqrt{\epsilon_{ii}\epsilon_{jj}}$ and $2\sigma_{ij} = \sigma_{ii} + \sigma_{jj}$ and $\mathbf{r}_{ij}$ is the distance vector between the $i$th atom of the molecule and the $j$th carbon atom.

In the second term of Eq. (1) $\mathbf{E}^{j}_{\mathrm{M}}$ is the field generated by the molecular permanent electric multipole moments ($\mu$, $\mathbf{\Theta}$,...) of the $NH_3$ molecule at position $\mathbf{r}_0$ on the $j$th carbon atom of the fullerene molecule at position $\mathbf{r}_j$ with polarizability tensor $\alpha^j$. It is expressed as

$$\mathbf{E}^{j}_{\mathrm{M}} = \nabla\nabla\left(\frac{1}{|\mathbf{r}_j - \mathbf{r}_0|}\right)\cdot\mu + \frac{1}{3}\nabla\nabla\nabla\left(\frac{1}{|\mathbf{r}_j - \mathbf{r}_0|}\right) : \mathbf{\Theta} + ... \tag{2}$$

Note that the multipole moments of $NH_3$ and the polarizability tensor of each carbon atom of $C_{60}$ are usually defined and given with respect to local frames with their origins at the centre of mass of $NH_3$ (G,**x**,**y**,**z**) or each carbon atom ($C_j$,$\mathbf{x}_j$,$\mathbf{y}_j$,$\mathbf{z}_j$) respectively. In the calculation, it is then necessary to express these quantities in an absolute frame (O,**X**,**Y**,**Z**) defined with respect to the fixed $C_{60}$ molecule. We use a transformation rotation matrix following Rose's convention [25] and given in Appendix B.

Figure 1 indicates how to describe the internal degrees of freedom of the molecule with respect to its frame (G,**x**,**y**,**z**) and its external orientational and translational degrees of freedom with respect to the absolute frame, and Table 1 gives the various fullerene and ammonia characteristic values used in our calculations.

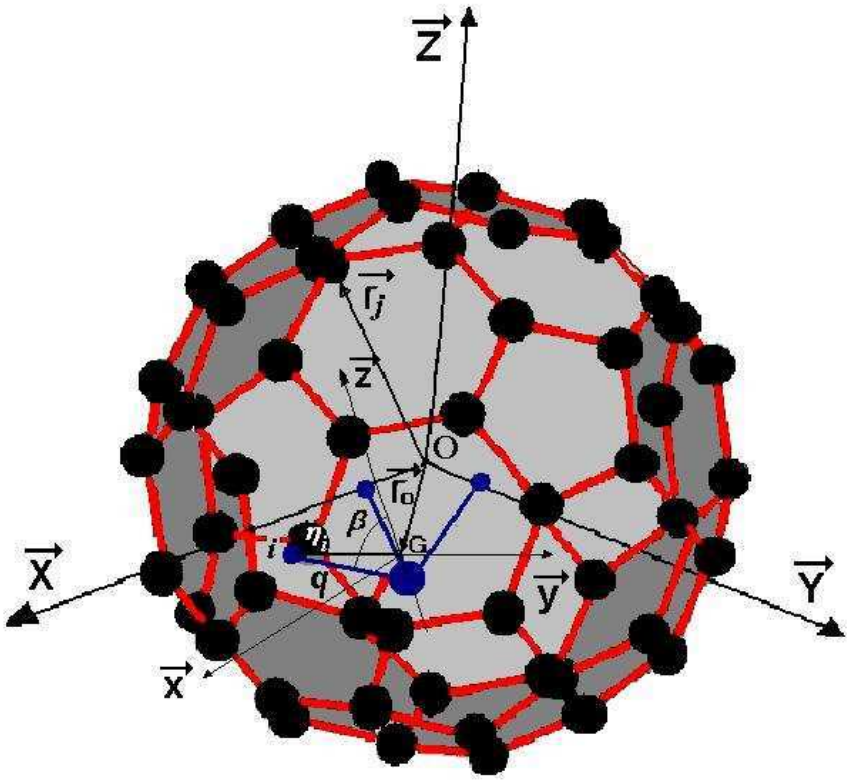


Figure 1: Geometrical characteristics of a molecule trapped in the fullerene molecule. (O,**X**,**Y**,**Z**) and (G,**x**,**y**,**z**) represent the absolute frame and the molecular frame, respectively. $q$ and $\beta$ define the equilibrium internal coordinates of the trapped molecule.

The distance vector $\mathbf{r}_{ij}$ in Eq.(1) can be expressed in terms of the position vectors $\mathbf{r}_0$ of the molecular centre of mass (c.m.) and $\mathbf{r}_j$ of the $j$th carbon atom of the fullerene molecule with respect to the absolute frame (O,**X**,**Y**,**Z**) and of the position vector $\eta_i$ of the $i$th atom of the molecule with respect to its associated frame (G,**x**,**y**,**z**):

$$\mathbf{r}_{ij} = \mathbf{r}_j - \mathbf{r}_0 - \eta_i, \tag{3}$$

The IR spectra of the trapped $NH_3$ molecule are usually given in terms of molecular vibrational $\{Q\}$ degrees of freedom.

Thus, to determine the influence of the surroundings on the molecular internal motions, the position vectors $\eta_i$ of the atoms in the molecule, the molecular dipole moment vector $\mu$, and the quadrupole

Table 1: Numerical parameters for $NH_3$ molecule and for $C_{60}$ molecule used in our calculations.

| $NH_3$ | | $C_{60}$ | |
|---|---|---|---|
| $q$ (Å) | 1.0156 | $R^{(a)}$ (Å) | 3.556 |
| $\beta$ (deg.) | 68. | d(C−C)$^{(a)}$ (Å) | 1.455 |
| | | d(C=C)$^{(a)}$ (Å) | 1.398 |
| $\mu^{\rm e}$ (D) | 1.476 | $\alpha^{\rm c}_{\perp}$ (Å$^3$) | 1.44 |
| $\Theta^{\rm e}$ (DÅ) | -2.930 | $\alpha^{\rm c}_{\parallel}$ (Å$^3$) | 0.41 |
| $B$ (cm$^{-1}$) | 9.941 | | |
| $C$ (cm$^{-1}$) | 6.309 | | |
| | C - C$^{(b)}$ | N - N$^{(c)}$ | H - H$^{(c)}$ |
| $\epsilon$ (cm$^{-1}$) | 19.4 | 26.5 | 17.2 |
| $\sigma$ (Å) | 3.40 | 3.38 | 2.53 |

($a$) From Ref. [26]. ($b$) From Ref. [27]. ($c$) From Ref. [36].

moment tensor $\mathbf{\Theta}$ can all be expressed in a series expansion with respect to the molecular frame in terms of the vibrational normal coordinates $\{Q\}$.

Taking only the first order terms gives

$$\begin{aligned} \eta_i &= \eta_i^{\rm e} + \sum_\nu \mathbf{a}_i^\nu Q_\nu, \\ \mu &= \mu^{\rm e} + \sum_\nu \mathbf{b}^\nu Q_\nu, \\ \mathbf{\Theta} &= \mathbf{\Theta}^{\rm e} + \sum_\nu \mathbf{c}^\nu Q_\nu. \end{aligned} \tag{4}$$

In these expressions $\eta_i^{\rm e}$ is the vector position of the $i$th atom in the rigid molecule, and $\mu^{\rm e}$ and $\mathbf{\Theta}^{\rm e}$ are its permanent multipole moments, while $\mathbf{a}_i^\nu$, $\mathbf{b}^\nu$, and $\mathbf{c}^\nu$ are the first derivatives of $\eta_i$, $\mu$, and $\mathbf{\Theta}$ with respect to the normal coordinate $Q_\nu$ which describes the $\nu$th molecular vibrational mode with frequency $\omega_\nu$. Note that the expression of $\mu$ will also be used in the near and far infrared spectra calculations.

However, it must be noticed that because of the *dual nature* of the $\nu_2$ mode of the ammonia molecule, that is, the *high frequency vibration-low frequency inversion*, this mode will be treated in a particular way.

Using the Born-Oppenheimer approximation (adiabatic approximation) to separate the high frequency vibrational modes $\{Q\}$ of the molecule from its low frequency external modes, that is, the orientation $\mathbf{\Omega} = (\varphi, \theta, \chi)$ and c.m. translation $\mathbf{r}_0$ motions, the interaction potential energy $V_{\rm MC}$ can be written as

$$V_{\rm MC} = V_{\rm M}(\mathbf{r}_0, \mathbf{\Omega}) + W_{\rm M}(\{Q\}) + \triangle V_{\rm M}(\mathbf{r}_0, \mathbf{\Omega}, \{Q\}), \tag{5}$$

where $V_{\rm M}(\mathbf{r}_0, \mathbf{\Omega})$ represents the low frequency motions dependent part of the potential energy for the non vibrating molecule, and $W_{\rm M}(\{Q\})$ characterizes the vibrational dependent part for the molecule at its equilibrium position and orientation, and is generally a small perturbation which involves only vibrational level shifts and/or splittings. It can be developed in a Taylor series expansion up to second order with respect to the vibrational normal coordinates $\{Q\}$ as

$$W_{\rm M}(\{Q\}) = \sum_\nu \frac{\partial V_{\rm MC}}{\partial Q_\nu} Q_\nu + \frac{1}{2} \sum_{\nu\nu'} \frac{\partial^2 V_{\rm MC}}{\partial Q_\nu \partial Q_{\nu'}} Q_\nu Q_{\nu'} + ... \tag{6}$$

Finally the third term in Eq.(5) characterizes the coupling between the external and the internal modes which can lead to the vibrational energy relaxation.

## 2.2 Potential energy surfaces

### 2.2.1 Orientation-translation motions

The first step of the numerical calculations consists in determining the equilibrium configuration of the rigid ammonia molecule into the $C_{60}$ cage. The potential energy $V_M$ (see Eq.(5) is minimized with respect to both the c.m. displacement vector $\mathbf{r}_0$ and the molecular orientional coordinates $\varphi$, $\theta$, and $\chi$.

We find that the equilibrium configuration has an energy minimum value of - 1460 $cm^{-1}$ for the $\mathbf{z}$ molecular axis (threefold symetry axis $C_3$) oriented along the direction connected to each two symmetrical carbon atoms. The c.m. is then displaced from the site centre by about 0.184 Å in the same direction. An energy maximum of - 1445 $cm^{-1}$ is obtained when the molecule is oriented and its c.m. displaced by 0.188 Å along the pentagon centre directions. There is also an intermediate energy value of - 1455 $cm^{-1}$ that is calculated for the molecule oriented and its c.m. displaced by 0.180 Å along the hexagon centre directions.

Thus, the calculations show that *i*) in all the molecular orientational configurations, the c.m. displacements $r_0$ have always opposite directions to the molecular $\mathbf{z}$ axis, and *ii*) the energy changes are negligibly small $\lesssim 3$ $cm^{-1}$ when $r_0$ changes by about 0.01 Å along these directions. So, in the following we will take the value $r_0^e = 0.184$ Å as a mean value for every orientation. This means that the trajectory of the molecular c.m. can be approximated by the surface of a sphere of radius $r_0^e$.

Note, moreover, that the induction and repulsion-dispersion contributions represent, respectively, 35% (- 498 $cm^{-1}$) and 65% (- 963 $cm^{-1}$) of the total energy.

As a result, the potential energy surface $V_M(r_0(\mathbf{\Omega}))$ is nearly flat since the barrier height is always $\lesssim$ 16 $cm^{-1}$ and the c.m. displacement vectors $\mathbf{r}_0$ from the cage centre remain always nearly anticollinear to the molecular $\mathbf{z}$ axis *i.e.* $\mathbf{z}\cdot\ \mathbf{r}_0 \simeq -\ r_0$. This is not surprising because of the repulsive character of the hydrogen atoms of the molecule and reflects a very strong coupling between its orientation and the location of its centre of mass.

Thus, on one hand, the axis of the molecule undergoes only oscillatory motions $(\varphi, \theta)$ of small amplitude around the direction of each displacement vector $\mathbf{r}_0^e$. The corresponding potential energy surface which is given in Figure 2 is a nearly harmonic two dimension librational oscillator. The associated frequencies are $\omega_\varphi \simeq 155$ $cm^{-1}$ and $\omega_\theta \simeq 151$ $cm^{-1}$.

On the other hand, for a given molecular orientation, the radial potential function $V_M(r_0)$ of the translation motion of the molecular c.m. around the equilibrium position $r_0^e = 0.184$ Å is plotted in Figure 3. The curve appears as that of a nearly harmonic one dimensional oscillator with a force constant value $k = 2.4\times10^4$ $cm^{-1}.Å^{-2}$ corresponding to a frequency $\omega_{rad} \simeq 218$ $cm^{-1}$.

On the basis of these features, we can conclude that ammonia should exhibit a nearly free rotation motion simultaneously around the centre of the cage by describing a spherical curve with radius $r_0^e =$ 0.184 Å, and around its centre of mass. Note however that the spinning motion $\chi$ remains around the threefold symmetry axis of the molecule, only.

Finally, it is clear that this rotation-c.m. translation motion is slow with respect to the librational and the radial motions and can be separated from the latter using the adiabatic approximation.

### 2.2.2 Inversion-translation motions

It is also clear, from the results above, that when the inversion motion of the molecule proceeds, its centre of mass moves simultaneously from one position $(\mathbf{r}_0^e, \mathbf{\Omega})$ to the opposite one $(-\mathbf{r}_0^e, \mathbf{\Omega})$ with respect to the cage centre where the molecule lies in its planar configuration.

### 2.2.3 Few remarks

It must be noticed that the interaction potential energy experienced by the ammonia molecule trapped in the fullerene molecule strongly depends on the geometrical characteristics such as the radius of the $C_{60}$ cage and the equilibrium internal coordinates ($q$,$\beta$ see Fig. 1) of the ammonia molecule, and also on the dispersion-repulsion potential parameters especially the Lennard-Jones $\sigma$ parameters.

For instance, in one hand, the minimum depth is enhanced from - 1460 to - 750 $cm^{-1}$ when the fullerene radius is decreased by 1%, from 3.556 to 3.519 Å, and it diminishes to - 2000 and - 2411 $cm^{-1}$

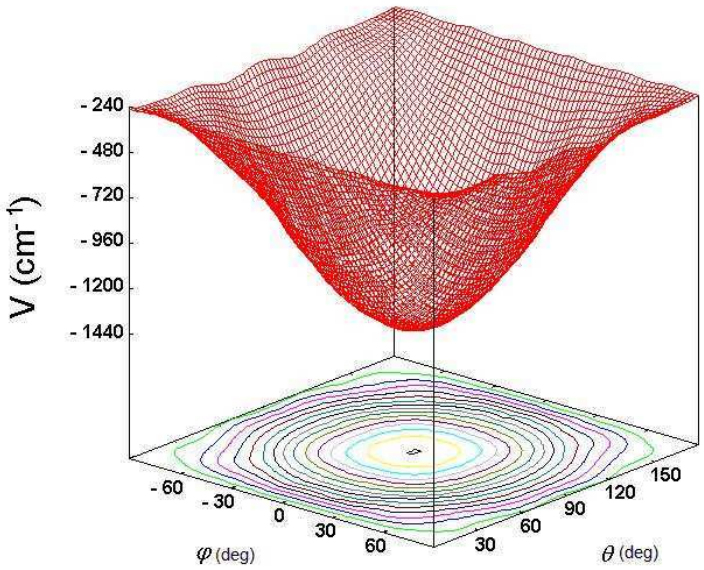


Figure 2: Potential energy surface *versus* $(\varphi, \theta)$ angular motions around the molecular equilibrium configuration $(\mathbf{r}_0^{\mathrm{e}}, \mathbf{\Omega})$.

when the radius value is increased by 1% and 2%, to 3.592 and 3.627 Å, respectively. The induction energy contribution undergoing only weakly variations.

In the other hand, changes of the $\sigma$ parameters of + 1% and - 1% involve, respectively, minimum depths of - 952 and - 1976 $\mathrm{cm}^{-1}$.

However, in spite of these changes in the well depth values, the potential energy surface $V_{\mathrm{M}}(\mathbf{r}_0^{\mathrm{e}}, \mathbf{\Omega})$ remains nearly flat since its barrier height does not exceed 24 $\mathrm{cm}^{-1}$. Furthermore, the potential energy surfaces associated with the various motions remain nearly unchanged.

Thus, from the previous analysis of the potential energy experienced by the ammonia molecule into the fullerene molecule, we will assume that the c.m. position vector $\mathbf{r}_0$ remains permanently anticollinear to the $\mathbf{z}$ molecular axis and separate it into a static position vector $\mathbf{r}_0^{\mathrm{e}}(\varphi, \theta, Q_2)$ which parametrically depends on the orientation and inversion degrees of freedom, and a dynamical coordinate $\mathbf{u}_0$ characterizing the c.m. vibration around $\mathbf{r}_0^{\mathrm{e}}(\varphi, \theta, Q_2)$.

Finally, it is clear that inversion-c.m. translation motions $(r_0^{\mathrm{e}}, Q_2)$, on one hand, and orientation-c.m. translation motions $(\mathbf{r}_0^{\mathrm{e}}, \mathbf{\Omega})$, on the other hand, are strongly coupled; their kinetic operator must be classically treated, as explained in appendix A, before their quantum mechanical treatment as described below. The interaction potential energy $V_{\mathrm{MC}}$ can be rewritten as

$$V_{\mathrm{MC}} = V_{\mathrm{M}}(\mathbf{r}_0^{\mathrm{e}}, \mathbf{\Omega}) + V_{\mathrm{M}}(r_0) + V_{\mathrm{M}}(r_0, Q_2) + W_{\mathrm{M}}(\{Q\}) + \triangle V_{\mathrm{M}}(\mathbf{r}_0, \mathbf{\Omega}, \{Q\}), \tag{7}$$

# 3 Quantum-classical model

As we have mentioned above, the purpose of this work is to determine the infrared spectra of the $NH_3$ molecule trapped in a rigid $C_{60}$ molecule. The Hamiltonian of the optically active molecule considered as

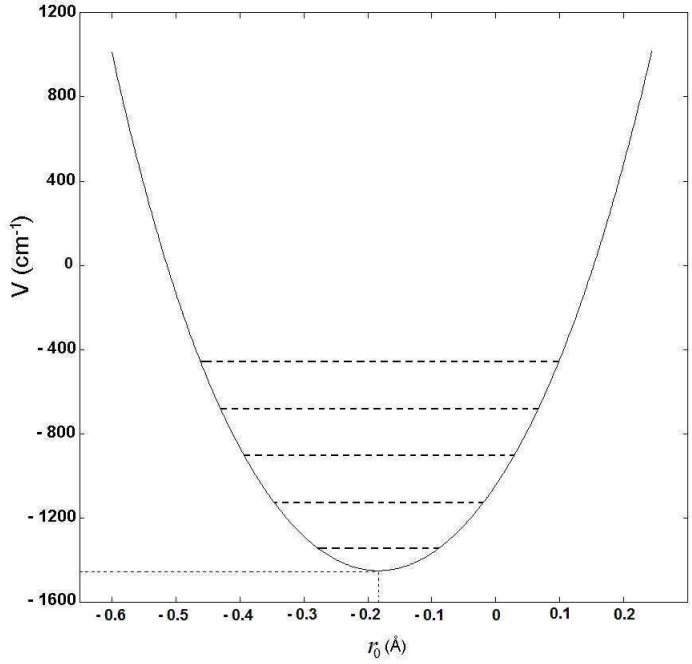


Figure 3: Potential energy function *versus* molecular c.m. displacement $r_0$ around its equilibrium position vector $\mathbf{r}_0^{\mathrm{e}}$.

quantum mechanical system can be expressed from the potential energy surfaces calculated above and the quantum mechanical model for the orientational and vibrational kinetic energy operators. The latter are obtained from the correspondence principle applied to the classical formulation described in Appendix A. Disregarding the dynamical couplings between the orientational and vibrational degrees of freedom the Hamiltonian can thus be written as

$$H_{\mathrm{a}}^{\mathrm{eff}} = H_{\mathrm{orient}}^{\mathrm{eff}} + H_{\mathrm{vib}}^{\mathrm{eff}}; \tag{8}$$

where $H_{\mathrm{orient}}^{\mathrm{eff}}$ and $H_{\mathrm{vib}}^{\mathrm{eff}}$ are, respectively, the renormalized Hamiltonians associated with the orientation and the vibration modes which account for the couplings ($\mathbf{r}_0^{\mathrm{e}}$,$\mathbf{\Omega}$) and ($r_0^{\mathrm{e}}$,$Q_2$).

## 3.1 The orientation modes

Following expressions derived in Appendix A, the quantum mechanical renormalized Hamiltonian $H_{\mathrm{orient}}^{\mathrm{eff}}$ for the non-vibrating molecule can be written as

$$H_{\mathrm{orient}}^{\mathrm{eff}} = T_{\mathrm{rot}}^{\mathrm{eff}} + V_{\mathrm{M}}(\mathbf{r}_0^{\mathrm{e}}, \mathbf{\Omega}); \tag{9}$$

where $T_{\mathrm{rot}}^{\mathrm{eff}}$ is the effective rotational kinectic operator

$$T_{\mathrm{rot}}^{\mathrm{eff}} = -B^{\mathrm{eff}} \left\{ \frac{\partial^2}{\partial\theta^2} + \cot\theta \frac{\partial}{\partial\theta} + \frac{1}{\sin^2\theta} \frac{\partial^2}{\partial\varphi^2} + \left( \cot^2\theta + \frac{C}{B^{\mathrm{eff}}} \right) \frac{\partial^2}{\partial\chi^2} - 2 \frac{\cot\theta}{\sin\theta} \frac{\partial^2}{\partial\varphi\partial\chi} \right\}. \tag{10}$$

In this equation $B^{\mathrm{eff}} = \hbar^2/2I_{\mathrm{B}}^{\mathrm{eff}}$ is the effective rotational constant connected to the rotation-c.m. translation motion of the $C_3$ symmetry axis for the trapped molecule and $C$ its rotational constant of the spinning motion around this axis for the gas-phase molecule $C = 6.309$ cm$^{-1}$. The value of $B^{\mathrm{eff}}$ is equal to 7.419 cm$^{-1}$ which is less than the gas-phase value of 9.941 cm$^{-1}$.

Furthermore, since the barrier height associated with the orientation-c.m. translation motion is always $\lesssim 16$ cm$^{-1}$, the potential $V_{\rm M}(\mathbf{r}_0^{\rm e}, \mathbf{\Omega})$ can be neglected. The renormalized Hamiltonian becomes $H_{\rm orient}^{\rm eff} \simeq T_{\rm rot}^{\rm eff}$.

The eigensolutions of this Hamiltonian are then $E_{JMK} = B^{\rm eff}J(J+1)+(C-B^{\rm eff})K^2$ for the eigenvalues (energy levels) and $|JMK\rangle$ for the eigenvectors where $J$, $M$, and $K$ are the usual quantum numbers connected to the free rotation motion of the ammonia molecule with the conditions $-J \leq M \leq +J$ and $-J \leq K \leq +J$. Note that these levels have $(2J+1)$-fold degeneracy on the quantum number $M$ and twofold degeneracy $(\pm)$ on the $K$ one, except when $K = 0$ [29]. The corresponding line structure of the far infrared (FIR) bar-spectrum is then identical to that of $NH_3$ gas-phase one.

## 3.2 The $\nu_2$ vibration-inversion mode

### 3.2.1 Gas-phase $NH_3$

In the vibration-inversion mode of the $NH_3$ molecule, the nitrogen atom can pass from one side of the plane defined by the three hydrogen atoms to the opposite one. This mode is generally described, to a good approximation, as one-dimension tunneling motion of one particle of mass equal to the reduced mass $\mu_2$ of $NH_3$ (2.563 g.mol$^{-1}$) moving in a symmetrical double-well potential function $V_{\nu_2}(Q_2)$ (left (L) and right (R) wells) as shown in Figure 4a, with a high but finite hindering barrier of 2047 cm$^{-1}$ [30], such as

$$V_{\nu_2}(Q_2) = \frac{1}{2}k_2Q_2^2 + A_2(\mathrm{e}^{-a_2Q_2^2} - 1); \tag{11}$$

where $k_2 = 58306$ cm$^{-1}$.Å$^{-2}$, $A_2 = 12469$ cm$^{-1}$ and $a_2 = 4.8224$ Å$^{-2}$.

The solution of such a problem leads to vibrational energy levels split into doublets, $(+)$ and $(-)$, due to inversion. The vibration-inversion wavefunctions are then described by $|v_2^{(\alpha)}\rangle$ $(\alpha = +, -)$, instead of $|v_2\rangle$, and are expressed as linear combinations (symmetric and antisymmetric) of the vibrational wavefunctions $|v_2^{(\rm L)}\rangle$ and $|v_2^{(\rm R)}\rangle$ associated with the left and right wells, respectively. Moreover, the only permitted transitions are $(+) \longleftrightarrow (-)$ as shown in Fig. 4a.

Note that the potential parameters given above were adjusted to give the fundamental frequency and the level splittings corresponding to the experimental values, that is, 950 cm$^{-1}$ for the frequency and 0.8 cm$^{-1}$ for $v_2 = 0$ and 35.8 cm$^{-1}$ for $v_2 = 1$ level splittings.

### 3.2.2 Trapped $NH_3$

When the $NH_3$ molecule is trapped in $C_{60}$ cage, the gas-phase double-well potential function is modified. In the calculations, the inversion-c.m. translation potential energy $V_{\rm M}(r_0, Q_2)$ (see Eq. (7)) is numerically added to the potential function $V_{\nu_2}(Q_2)$ of Eq. (11). The new double-well potential function is shown in Fig. 4b as a function of the inversion angular coordinate. Its symmetry is preserved but the hindering barrier is increased by 404 cm$^{-1}$. Moreover, from expressions given in Appendix A, the effective reduced mass is equal to $\mu_2^{\rm eff} = 6.569$ g.mol$^{-1}$ leading to an increase of 156% with respect to the gas-phase value of 2.563 g.mol$^{-1}$.

The corresponding Schrödinger equation was solved numerically using a discrete variable representation method [37]. The computed level scheme is given in Fig. 4b.

In gas-phase, the $\nu_2$ mode is measured at 931.7 cm$^{-1}$ and 968.3 cm$^{-1}$. In $C_{60}$, it is shifted by 47.0 cm$^{-1}$ (as given below) and because the double-well inversion potential is modified with an increase in the hindering barrier height and the effective reduced mass as discussed above, this mode is quasi-degenerate and is calculated at 751.6 cm$^{-1}$, that is, (704.6+47.0) cm$^{-1}$ (see Fig. 4b). This result is to be related to an increase in the tunneling time for both the fundamental and the first excited levels in $C_{60}$, since the values are equal to 20.85 ps and 0.47 ps in gas-phase compared to 55594 ps and 333.56 ps in $C_{60}$, respectively. We can infer from these results that in $C_{60}$, localization of the N atom occurs in one of the wells of the potential function and that the $\nu_2$ mode is quasi-degenerate.

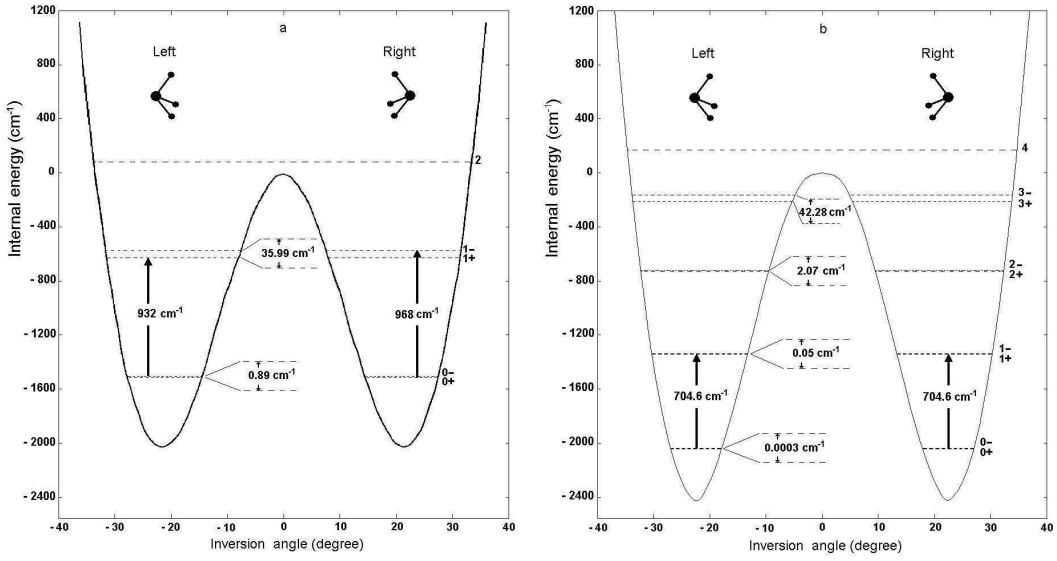


Figure 4: Vibration-inversion double-well potential energy of $NH_3$ as a function of the angle between the N−H bond and the plane of the H atoms. The obtained energy levels and the allowed fundamental transitions are also shown (a) for the gas-phase and (b) for the trapped one in the fullerene nano-cage.

### 3.3 The vibrational frequency shifts

The second term of Eq. (8) is the renormalized vibrational Hamiltonian which accounts for the vibrational dependent part $W_{\rm M}(\{Q\})$ and inversion-c.m. translation part $V_{\rm M}(r_0, Q_2)$ of the interaction potential energy

$$H_{\rm vib}^{\rm eff} = H_{\rm vib} + W_{\rm M}(\{Q\}) + V_{\rm M}(r_0, Q_2); \tag{12}$$

where $H_{\rm vib}$ characterizes the gas-phase molecular vibrational Hamiltonian written as

$$H_{\rm vib} = \sum_{\nu} \frac{P_\nu^2}{2\mu_\nu} + \frac{1}{2}\sum_{\nu} k_\nu Q_\nu^2 + \triangle V_{\rm vib}^{\rm anh}(\{Q\}). \tag{13}$$

In this expression $\mu_\nu$ and $k_\nu$ are, respectively, the reduced mass and the harmonic force constant connected to the $\nu$th vibrational mode, with associated normal coordinate $Q_\nu$ and conjugate momentum $P_\nu$, and $\triangle V_{\rm vib}^{\rm anh}(\{Q\})$ represents the anharmonic part of the internal potential function. The eigenelements of this Hamiltonian $H_{\rm vib}$ have previously been obtained from the *ab initio* calculations of Martin *et al.* [28].

Let $E_{v_\nu}$ and $|...v_\nu...\rangle$ be the eigenvalues and eigenvectors of the $v$th level associated with the $\nu$th vibrational mode.

Thus, a first order perturbation treatment allows us to determine the frequency shift $\Delta\omega_\nu$ associated with the vibrational fundamental transition $|\ ...0_\nu...\rangle \rightarrow |\ ...1_\nu...\rangle$ for the trapped molecule from the equation

$$\Delta\omega_\nu = \hbar^{-1}\left[\langle ...1_\nu... \mid W_{\rm M}(\{Q\}) \mid ...1_\nu...\rangle - \langle ...0_\nu... \mid W_{\rm M}(\{Q\}) \mid ...0_\nu...\rangle\right]; \tag{14}$$

in which all other modes remain in their fundamental states and $\hbar = h/2\pi$. The computed values are given in Table 3. We note that each of the vibrational modes are blue shifted with splitting of the degenerate levels of $\nu_3$ mode (strong) and $\nu_4$ mode (weak) modelled from static effect. Whereas for degenerate $\nu_2$ mode the blue shift of 47.0 $\rm cm^{-1}$ from static effect, is modified to red shift when dynamic effect on 1D tunneling motion of the N atom is considered as discussed above.

Table 2: Vibrational frequency shifts ($cm^{-1}$) of $NH_3$ molecule trapped in the $C_{60}$ cage, together with the gas-phase frequencies.

| Vibrational modes | Frequency shifts ($cm^{-1}$) | Gas-phase frequencies ($cm^{-1}$) |
|---|---|---|
| $\nu_1$ | 133.0 | 3337 |
| $\nu_2$ | 47.0 | 950 |
| $\nu_{3a}$ | 171.0 | 3448 |
| $\nu_{3b}$ | 69.6 | |
| $\nu_{4a}$ | 47.1 | 1627 |
| $\nu_{4b}$ | 34.0 | |

# 4 Infrared absorption spectra

## 4.1 General

The infrared absorption coefficient for the optically active ammonia molecule trapped in a $C_{60}$ fullerene molecule at temperature $T$, is defined as the real part of the spectral density, *i.e.*, the Fourier transform of the time-dependent autocorrelation function $\phi(t)$

$$\begin{aligned} I(\omega) &= \frac{4\pi\mathcal{N}\omega}{3hc}\mathrm{Re}\int_0^\infty dt e^{i\omega t}\phi(t), \\ \phi(t) &= \mathrm{Tr}\left[\rho(0)\mu_A(0)\mu_A(t)\right], \end{aligned} \tag{15}$$

where $\omega$ is a running frequency variable and $c$ the speed of light, $\rho(0)$ characterizes the initial canonical density matrix operator of the system, and $\mu_A$ is the molecular dipole moment operator defined in the absolute frame (see Appendix B). The trace (Tr) operation means an average over the initial conditions at time $t = 0$ and over all the possible evolutions of the system between times 0 and $t$.

However, since this work is devoted to constructing the infrared bar-spectra of the trapped ammonia molecule, we assume the *initial chaos hypothesis* for the density matrix to be valid. This allows us to write the optical wave functions $\mid v_\nu JMK\rangle$ as products of the renormalized vibrational and orientational ones $\mid v_\nu\rangle \otimes |JMK\rangle_{v_\nu}$. It must be noticed that the orientational states parametrically depend on the vibrational states through the moments of inertia. This dependence will be ignored below.

## 4.2 Near infrared bar-spectrum

Within this framework, the infrared bar-spectrum connected to the $\nu$th fundamental vibrational mode transition $\mid 0_\nu\rangle \longrightarrow \mid 1_\nu\rangle$ (all other modes being in their fundamental states) is written in the Lorentzian form as

$$I_\nu(\omega) = \frac{8\pi^2\mathcal{N}}{3hc}\omega\left|\langle 0_\nu|Q_\nu|1_\nu\rangle\right|^2 \sum_{JMKJ'M'K'} \frac{e^{-\beta E_{0JMK}} - e^{-\beta E_{1J'M'K'}}}{Z}\left|\left\langle JMK\left|\frac{\partial\mu_A}{\partial Q_\nu}\right|J'M'K'\right\rangle\right|^2 \times\delta\left(\omega - \omega_{0JMK\to 1J'M'K'} - \Delta\omega_\nu\right). \tag{16}$$

In this equation the $\langle ...\rangle$ brackets refer to vibrational transition elements of the normal coordinate $Q_\nu$ and to the orientational transition elements of the first derivative of the molecular dipole moment with respect to this coordinate. The numerical values connected to all the $NH_3$ modes are given in Appendix B. Moreover, $Z$ defines the orientation canonical partition function associated with the fundamental vibrational level at temperature $T$, $\beta = (k_B T)^{-1}$ where $k_B$ is the Boltzmann's constant, $\delta$ is the Dirac's function, and $\omega_{0JMK\to 1J'M'K'} = \hbar^{-1}\left(E_{1J'M'K'} - E_{0JMK}\right)$ is the transition frequency. Note that we use below the usual spectroscopic nomenclature to designate the line transitions connected to the rotational selection rules, that is, $Q(J_K)$ for $\Delta J = 0$, $R(J_K)$ for $\Delta J = +1$, and $P(J_K)$ for $\Delta J = -1$.

### 4.3 $\nu_2$ mode results and discussion

In Figure 5, are given the near infrared bar-spectra of $NH_3$ trapped in fullerene in the $\nu_2$ mode absorption region for three different temperatures, 10 K, 30 K and 100 K. The spectra are calculated by taking into account the frequency shift and allowed rovibrational transition elements following selection rules.

For the latter, as the first derivative of the molecular dipole moment with respect to the $Q_2$ coordinate does not depend on the rotational spinning angle $\chi$, $\Delta K = 0$ for the $K$ quantum number.

The infrared bar-spectrum consists of a Q line located at the pure vibration-inversion frequency 751.6 $cm^{-1}$, and a set of rotation-vibration-inversion lines P and R 14.8 $cm^{-1}$ apart, corresponding to $2B^{\text{eff}}$, on both sides of the Q branch.

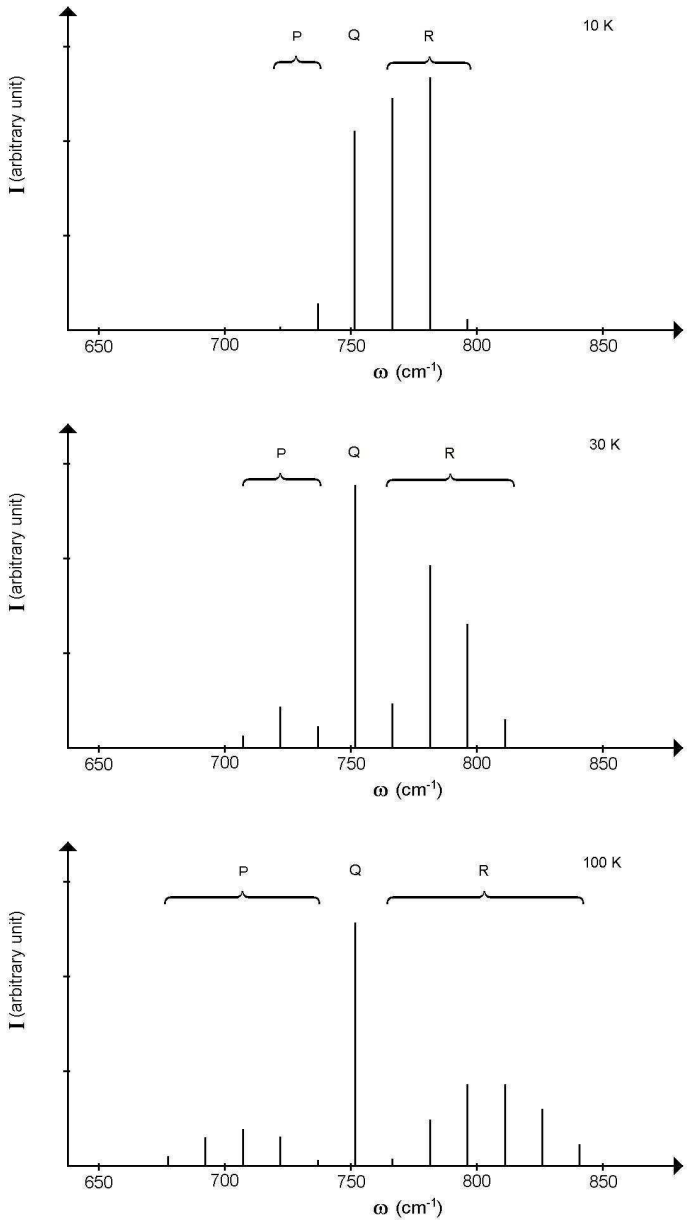


Figure 5: Near infrared bar-spectrum in the $\nu_2$ vibration-inversion frequency region for $NH_3$ trapped in the fullerene nano-cage at temperatures 10, 30 and 100 K.

At $T = 10$ K, only the lowest few rotational states are populated. As a result, the bar-spectrum shown

in Figure 5a exhibits only three lines: *i*) a Q line at 751.6 $cm^{-1}$ which is in fact a superposition of the three transitions $Q(1_1)$, $Q(2_1)$ and $Q(2_2)$, *ii*) a $R(0_0)$ line at 766.4 $cm^{-1}$ and *iii*) a R line, superposition of $R(1_0)$ and $R(1_1)$ lines at 781.3 $cm^{-1}$. There is only one $P(1_0)$ line located at 736.8 $cm^{-1}$.

As the temperature increases, more and more rotational states are populated and as result, more lines appear in the spectra with a different distribution in terms of intensities. At 30 K, the Q line is the most intense consisting of a superposition of $Q(J_K)$ lines for $J = 1$ to 4 and $1 \leq K \leq J$. Moreover, the intensity of lines $R(0_0)$ and $R(1_K)$ decreases leading to the increase of the $R(2_K)$ line which is located at 796.1 $cm^{-1}$. More lines appear in the R and P branches ($R(3_K)$ and $P(2_K)$).

At 100 K, the Q branch consists of a superposition of 6 lines for $J$ varying from 1 to 6. The R and P branches are broader with lines of weaker intensities than those at 10 and 30 K in particular for the maxima.

The modification of the spectra near $\nu_2$ with temperature shows that the spectral signature of the trapped molecule can be used to sense the environmental temperature of fullerene $C_{60}$. As the coupling with the vibrational modes of $C_{60}$ is weak, the signal to noise ratio may be high enough for all the lines to be observed. In our opinion this result can be extrapolated to other types of simple molecules trapped in $C_{60}$.

Finally, the dynamical coupling of the vibration-rotation states of the $NH_3$ molecule with the vibrational modes of fullerene $C_{60}$ involves well separated states for the latter. As a result, this coupling is weak and the energy from local translational modes cannot redistribute itself in the thermal bath of $C_{60}$. The linewidths are then negligible.

In conclusion, this work shows that the simulation of the spectra of $NH_3$ can be used to probe the temperature of the media in which fullerene is observed. This result can probably be extended to other molecules trapped in fullerene, in particular when the coupling with the vibration modes of fullerene is weak, because signal to noise ratio should then be high enough for the rotation lines to be observed.

**ACKNOWLEDGEMENTS**

The authors thank the Regional Councels of Franche-Comté and Ile de France, the General Councel of the 78$^{\text{th}}$ district of Yvelines, the DGCIS from Ministry of Industry in France, the MOVEO cluster for financing the FUI project MEMOIRE under the label of cluster MOVEO, CNRS for financing support under the Interdisciplinary Research Program of the INSU "Planetary Environments and Life Origins (EPOV)", and also Camille Lakhlifi for figures help.

# A Kinetic Lagrangian expression

The kinetic Lagrangian associated with the ammonia inversion, orientation, and c.m. translation modes considered as classical motions is

$$L_{\rm K} = \frac{1}{2}\mu_2 \dot{Q_2}^2 + \frac{1}{2} I_{\rm B}(\dot{\theta}^2 + \dot{\varphi}^2 \sin^2\theta) + \frac{1}{2} I_{\rm C}(\dot{\varphi}\cos\theta + \dot{\chi})^2 + \frac{1}{2} M \dot{r}_0^2, \tag{17}$$

where $\mu_2$ is the reduced mass of the molecule associated with the $\nu_2$ mode, $I_{\rm B}$ and $I_{\rm C}$ are the molecular principal moments of inertia for the rotation motion of its $C_3$ symmetry axis and the spinning motion around this axis, respectively, and $M$ is the molecular mass. Moreover, as it has been mentioned above, the position vector of the centre of mass of the molecule can be written as $\mathbf{r}_0 = \mathbf{r}_0^{\rm e}(\varphi, \theta, Q_2) + \mathbf{u}_0$. The velocity vector $\dot{\mathbf{r}}_0$ is then

$$\dot{\mathbf{r}}_0 = (\frac{\partial \mathbf{r}_0^{\rm e}}{\partial \varphi}\dot{\varphi} + \frac{\partial \mathbf{r}_0^{\rm e}}{\partial \theta}\dot{\theta} + \frac{\partial \mathbf{r}_0^{\rm e}}{\partial Q_2}\dot{Q}_2) + \dot{\mathbf{u}}_0. \tag{18}$$

By substituting Eq. (18) into Eq. (17), this latter equation becomes

$$L_{\rm K} = \frac{1}{2}\mu_2^{\rm eff} \dot{Q_2}^2 + \frac{1}{2} I_{\rm B}^{\rm eff}(\dot{\theta}^2 + \dot{\varphi}^2 \sin^2\theta) + \frac{1}{2} I_{\rm C}(\dot{\varphi}\cos\theta + \dot{\chi})^2 + \frac{1}{2} M \dot{u}_0^2 + M \frac{\partial r_0^{\rm e}}{\partial Q_2}\dot{Q}_2 \dot{u}_0, \tag{19}$$

where $\mu_2^{\rm eff}$ and $I_{\rm B}^{\rm eff}$ are effective reduced mass and moment of inertia

$\mu_2^{\rm eff} = \mu_2 + M\left(\frac{\partial r_0^{\rm e}}{\partial Q_2}\right)^2$, and $I_{\rm B}^{\rm eff} = I_{\rm B} + M {r_0^{\rm e}}^2$.

Note that the last term in Eq. (19) accounts for the simultaneous dynamical evolution of the translation motion of the centre of mass of the molecule and its inversion motion.

# B Rotational matrix transformation and molecular dipole moment

The unitary matrix $\mathbf{M}$ characterizing the transformation from the absolute frame (O,$\mathbf{X}$,$\mathbf{Y}$,$\mathbf{Z}$) into the molecular one (G,$\mathbf{x}$,$\mathbf{y}$,$\mathbf{z}$) through the Euler angles $\varphi$, $\theta$ and $\chi$ is given as [25]

$$\mathbf{M}(\varphi,\theta,\chi) =$$

$$\begin{pmatrix} \cos\varphi\cos\theta\cos\chi - \sin\varphi\sin\chi & \sin\varphi\cos\theta\cos\chi + \cos\varphi\sin\chi & -\sin\theta\cos\chi \\ -\cos\varphi\cos\theta\sin\chi - \sin\varphi\cos\chi & -\sin\varphi\cos\theta\sin\chi + \cos\varphi\cos\chi & \sin\theta\sin\chi \\ \cos\varphi\sin\theta & \sin\varphi\sin\theta & \cos\theta \end{pmatrix}. \tag{20}$$

Thus, the molecular dipole moment $\mu_A$ and its first derivative vectors $\frac{\partial \mu_A}{\partial Q_\nu}$, with respect to the normal coordinate $Q_\nu$ of the $\nu$th vibrational mode can be written in the absolute frame as

$$\begin{aligned} \mu_A &= \mathbf{M}^{-1}(\varphi,\theta,\chi)\mu, \\ \frac{\partial \mu_A}{\partial Q_\nu} &= \mathbf{M}^{-1}(\varphi,\theta,\chi)\mathbf{b}^\nu, \end{aligned} \tag{21}$$

where $\mathbf{M}^{-1}$ is the inverse matrix of $\mathbf{M}$, and $\mathbf{b}^{\nu} = \frac{\partial \mu}{\partial Q_{\nu}}$ the first derivative vectors of the molecular dipole moment expressed in the molecular frame. Their non vanishing component values (in D$\mathrm{\AA}^{-1}$) are [38]

$$\left\{ \begin{array}{ll} \mathrm{b}^{1} = \frac{\partial \mu_z}{\partial Q_1} = 1.404 & \mathrm{b}^{2} = \frac{\partial \mu_z}{\partial Q_2} = -4.409 \\ \mathrm{b}^{3a} = \frac{\partial \mu_x}{\partial Q_{3a}} = -4.012 & \mathrm{b}^{3b} = \frac{\partial \mu_y}{\partial Q_{3b}} = 2.465 \\ \mathrm{b}^{4a} = \frac{\partial \mu_x}{\partial Q_{4a}} = 1.984 & \mathrm{b}^{4b} = \frac{\partial \mu_y}{\partial Q_{4b}} = -2.559 \end{array} \right\}.$$

Moreover, the values of the elements of the normal coordinates connected to the fundamental vibrational transitions are (in Å)

$$\left\{ \begin{array}{l} |\langle 0_1 \, | Q_1 | \, 1_1 \rangle| = 0.042 \\ |\langle 0_2 \, | Q_2 | \, 1_2 \rangle| = 0.069 \\ |\langle 0_3 \, | Q_3 | \, 1_3 \rangle| = 0.029 \\ |\langle 0_4 \, | Q_4 | \, 1_4 \rangle| = 0.060 \end{array} \right\}.$$

# References


[1] http://www.nasa.gov/mission_pages/spitzer/news/spitzer20100722.html

[2] J. Cami, J. Bernard-Salas, E. Peeters, and S. E. Malek, Science **329** (2010) 1180.

[3] H. W. Kroto, J. R. Heath, S. C. O'Brien, R. F. Curl, and R. E. Smalley, Nature **318** (1985) 162.

[4] C. Girardet and A. Lakhlifi, J. Chem. Phys. **91** (1989) 1423.

[5] P. R. Dahoo, I. Berrodier, V. Raducu, J. L. Teffo, A. Lakhlifi, and L. Abouaf-Marguin, Eur. Phys. J. D. **5** (1999) 71.

[6] P. R. Dahoo, A. Lakhlifi, H. Chabbi, and J. M. Coanga, J. Mol. Struct. **786** (2006) 157.

[7] D. S. Bethune, R. D. Johnson, J. R. Salem, M. S. de Vries, and C. S. Yannoni, Nature **366** (1993) 123.

[8] H. Schwarz, T. Weiske, D. K. Böhme, and J. Hrušák, in: W. E. Billups and M. A. Ciufolini (Eds.), Buckminsterfullerenes, VCH Publishers, New York, 1993, Chap 10.

[9] M. Saunders, H. A. Jiménez-Vazquez, R. J. Cross, and R. J. Poreda, Science **259** (1993) 148.

[10] H. A. Jiménez-Vazquez, R. J. Cross, M. Saunders, and R. J. Poreda, Chem. Phys. Lett. **229** (1994) 111.

[11] M. Saunders, H. A. Jiménez-Vazquez, R. J. Cross, S. Mroczkowski, M. L. Gross, and D. E. Giblin, J. Am. Chem. Soc. **116** (1994) 2193.

[12] R. Shimshi, R. J. Cross, and M. Saunders, J. Am. Chem. Soc. **119** (1997) 1163.

[13] R. J. Cross, A. Khong, and M. Saunders, J. Org. Chem. **68** (2003) 8281.

[14] J. Cioslowski, J. Am. Chem. Soc. **113** (1991) 4139.

[15] C. I. Williams, M. A. Whitehead, and L. Pang, J. Phys. Chem. **97** (1993) 11652.

[16] J. Hernández-Rojas, J. Bretón, and J. M. Gomez Llorente, J. Chem. Phys. **104** (1996) 1179.

[17] J. Hernández-Rojas, J. Bretón, and J. M. Gomez Llorente, J. Chem. Phys. **104** (1996) 5754.

[18] E. H. T. Olthof, A. van der Avoird, and P. E. S. Wormer, J. Chem. Phys. **104** (1996) 832.

[19] R. J. Cross, J. Phys. Chem. A **112** (2008) 7152.

[20] M. Xu, F. Sebastianelli, Z. Bačić, R. Lawler, and N. J. Turro, J. Chem. Phys. **128** (2008) 011101.

[21] M. Xu, F. Sebastianelli, Z. Bačić, R. Lawler, and N. J. Turro, J. Chem. Phys. **129** (2008) 064313.

[22] Z. Slanina, F. Uhlík, L. Adamowicz, and S. Nagase, Mol. Simul. **31** (2005) 801.

[23] Ş. Erkoç and L. Türker, J. Mol. Struct. **640** (2003) 57.

[24] M. D. Ganji, M. Mohseni, and O. Goli, J. Mol. Struct. **913** (2009) 54.

[25] M. R. Rose, Elementary Theory of Angular Momentum, Wiley, New York, 1967.

[26] K. Hedberg, L. Hedberg, D. Bethune, C. A. Brown, H. C. Dorn, R. D. Johnson, and M. de Vries, Science **254** (1991) 410.

[27] H. Y. Song and X. W. Zha, Phys. Lett. A **373** (2009) 1058.

[28] J. M. L. Martin, T. J. Lee, and P. R. Taylor, J. Chem. Phys. **97** (1992) 8361.

[29] C. H. Townes and A. L. Schawlow, Microwave Spectroscopy, McGraw-Hill, London, 1955.

[30] J. D. Swalen and J. A. Ibers, J. Chem. Phys. **36** (1962) 2172.

[31] C. Girardet and A. Lakhlifi, J. Chem. Phys. **83** (1985) 550.

[32] A. Lakhlifi and C. Girardet, J. Mol. Spectrosc. **116** (1986) 33.

[33] C. Girardet and A. Lakhlifi, Chem. Phys. **110** (1986) 447.

[34] A. Lakhlifi and C. Girardet, J. Chem. Phys. **87** (1987) 4559.

[35] C. Girardet and A. Lakhlifi, J. Chem. Phys. **91** (1989) 2172.

[36] A. Lakhlifi, Euro. Phys. J. D **8** (2000) 211.

[37] J. C. Light, I. P. Hamilton, and J. V. Lill, J. Chem. Phys. **82** (1985) 1400.

[38] A. Lakhlifi and J. P. Killingbeck, J. Phys. Chem. B **109** (2005) 11322.